UNITED NATIONS EDUCATIONAL, SCIENTIFIC AND CULTURAL ORGANIZATION
INTERNATIONAL ATOMIC ENERGY AGENCY
INTERNATIONAL CENTRE FOR THEORETICAL PHYSICS
I.C.T.P., P.O. BOX 586, 34100 TRIESTE, ITALY, CABLE: CENTRATOM TRIESTE

SMR.959 - 25

MINIWORKSHOP ON STRONG ELECTRON CORRELATIONS
"Disorder and Interaction in Quantum Systems and Their Classical Analogs"

(1 - 19 July 1996)

"Magnetic Fluctuations in the Normal State of the High-T_c Superconductor $La_{1.86}Sr_{0.14}CuO_4$"

Gabriel Aeppli
N.E.C. Research Institute
4 Independence Way
Princeton, NJ 08540
U.S.A.

These are preliminary lecture notes, intended only for distribution to participants.

Magnetic Fluctuations in the Normal State of the High-T_c Superconductor $La_{1.86}Sr_{0.14}CuO_4$

G. Aeppli,[1,2] *T. E. Mason,*[2,3] *S. M. Hayden,*[4] *and H. A. Mook*[5]

[1] AT&T Bell Laboratories, Murray Hill, NJ 07974

[2] Risó National Laboratory, DK-4000 Roskilde, Denmark

[3] Dept. of Physics, University of Toronto, Toronto, Canada M5S 1A7

[4] Dept. of Physics, University of Bristol, Bristol BS8 1TL, United Kingdom

[5] Oak Ridge National Laboratory, Oak Ridge, TN 37831

ABSTRACT

We use neutron scattering to measure the magnetic response near (π,π) in the normal state (from T_c = 35 to 350 K) of superconducting single crystals of $La_{1.86}Sr_{0.14}CuO_4$. The incommensurate peaks which dominate the response have amplitudes which decrease as $1/T^2$ and widths which increase in proportion to $k_B T$ and energy transfer added in quadrature. For T > 100K, the observed peaks contain insufficient weight to account for the ^{63}Cu as well as planar ^{17}O nuclear relaxation rates.

PACS numbers: 74.72.Dn, 74.25.Ha, 61.12.Ex

MAY-29-1996 15:16 THEORETICAL PHYSICS 416 978 2537 P.11

The normal state of the metallic cuprates is as unusual as their superconductivity. For example, the electrical resistivity of samples with optimal superconducting properties is linear in temperature (T) from above 1000K to T_c.[1] Correspondingly, optical data reveal charge fluctuations with a characteristic energy scale which is simply $k_B T$.[1,2] Furthermore, the Hall number is strangely T-dependent, but in such a way as to give a Hall angle which varies as T^{-2}.[3] Finally, nuclear resonance[4,5] and bulk experiments[6] give an array of magnetic susceptibilities with qualitatively different T-dependences, which are not obviously related to the surprisingly simple behavior of the bulk and optical data. Of course, none of these measurements yields an image of the momentum (Q) and frequency (ω)-dependent magnetic response, $\chi''(Q,\omega)$. Magnetic neutron scattering, with a cross-section directly proportional to $\chi''(Q,\omega)$, does precisely this. It has established the detailed T-dependence of $\chi''(Q,\omega)$ both around T_c for samples doped to achieve optimal superconducting properties and over much larger temperature ranges for samples close to the metal-insulator transition.[7] However, relatively little has been done to characterize the normal state of the best superconductors, even though it is here where the oddity of the normal state is most obvious. In this paper, we describe neutron scattering experiments to measure the T-dependence of $\chi''(Q,\omega)$ in the normal state of $La_{2-x}Sr_xCuO_4$ with $x=0.14$ very near the optimal doping level (0.15) for this alloy, whose fundamental constituents are individual CuO_2 layers. As described previously,[8] the dominant features of $\chi''(Q,\omega)$ at low ω are four incommensurate peaks near $Q = (\pi,\pi)$, the magnetic ordering vector[9] of the parent insulator, La_2CuO_4. The important new results, which could not be anticipated from ref. (8), are

MAY-29-1996 15:16 THEORETICAL PHYSICS 416 978 2537 P.12

(i) that the effects of heating and raising $\hbar\omega$ on the peak widths in momentum space are indistinguishable, (ii) that, within error, the low ω peak susceptibilities vary as T^{-2} between T_c (35K) and 350K, and (iii) that the incommensurate peaks do not carry sufficient weight to account for the copper nuclear relaxation at high T.

The $La_{1.86}Sr_{0.14}CuO_4$ crystals and neutron spectrometer (TAS VI of the Risø DR3 Reactor) used in the present work are the same as those used in our previous determination[10] of $\chi''(Q,\omega)$ around and below the superconducting transition at T_c = 35K. Fig. 1 summarizes our surveys of $Q-\omega$ space at various temperatures. Frame (a) shows scans through the incommensurate peaks at $(\pi(1-\delta),\pi)$ and $(\pi,\pi(1+\delta))$ for energy transfer $\hbar\omega$ fixed at 6.1 meV. The important result is that the sharp peaks at 80K broaden to nearly merge at 297K. Frame (b) is an image of the scattering at $\hbar\omega$=6.1 meV and T=297K. Again, it is clear that the four peaks which characterize the low-temperature response near (π,π) have merged into an object whose boundary is roughly the square defined by the four low-T peaks. Finally, frames (c) - (e) illustrate the Q- and $\omega-$dependence of $\chi''(Q,\omega)$ determined using the fluctuation dissipation theorem, $\chi''(q,\omega)$ $(n(\omega)+1) = S(Q,\omega)$. The magnetic structure function S(Q, ω) is simply the scattering near the incommensurate peaks measured along the solid line in frame (b) and indicated by the filled symbols in (a), minus the background indicated by the open symbols in (a). Comparison of (c) and (d) shows that warming from T_c (35K) to 80K results in modest broadening of the magnetic peaks at low $\hbar\omega$, as well as an intensity reduction which is much more pronounced at low than at high $\hbar\omega$. Further warming to 297K (frame (e)) gives a much smaller $\chi''(Q,\omega)$, and eliminates clear incommensurate peaks at all $\hbar\omega$

MAY-29-1996 15:17 THEORETICAL PHYSICS 416 978 2537 P.13

probed. The dramatic T-dependent decrease of the $\chi''(Q,\omega)$ extracted from our data as well as its smooth variation from low to medium $\hbar\omega$ make significant phonon contamination of the background-corrected data very unlikely.

The defining features of $\chi''(Q,\omega)$ at a particular ω and T are the positions, widths, and intensities of the incommensurate peaks. Thus, we have parametrized our data at each $\hbar\omega$ and T in terms of the convolution of the instrumental resolution and the very general form,[11]

$$S(Q,\omega) = (n(\omega)+1)\chi''(Q,\omega) = \frac{(n(\omega)+1)\chi_P''(\omega,T)\kappa^4(\omega,T)}{(\kappa^2(\omega,T)+R(Q))^2} \quad . \qquad (1)$$

R(Q) is a function, with the full symmetry of the reciprocal lattice, which is everywhere positive except at zeroes coinciding with the incommensurate peak positions. From this definition, it follows that $\chi_P''(\omega,T)$ (in absolute units via a standard phonon-based calibration[12]) is the peak intensity and $\kappa(\omega,T)$ is an inverse length scale measuring the sharpness of the peaks. To perform fits, we have expanded R(Q) near (π,π) to lowest order in q_x and q_y, the components of Q relative to (π,π),

$$R(Q) = \frac{((q_x-q_y)^2-(\pi\delta)^2)^2 + ((q_x+q_y)^2-(\pi\delta)^2)^2}{2(2a_o\pi\delta)^2}, \qquad (2)$$

where $a_o = 3.8\text{Å}$ is the separation between nearest neighbor Cu atoms. Because all of our data show features at the low-T and $-\omega$ incommensurate positions, we simply fix δ at its low-T and $-\omega$ value of 0.245. The solid lines in Fig. 1(a) and the contours below the $\xi(\pi,\pi)$ line in Fig. 1(b) correspond to eq. (1) with parameters $\kappa(\omega,T)$ and $\chi_P''(\omega,T)$

chosen to obtain the best fit; that the data and fits are indistinguishable anests to the adequacy of eq. (1) as a description of our measurements.

The strategy for the remainder of this paper is to discuss $\kappa(\omega,T)$ and $\chi_p''(\omega,T)$ independently, search for obvious patterns in their T- and ω-dependence, and then to combine them to calculate the contribution of the incommensurate peaks to the nuclear relaxation rates. Fig. 2 shows how the inverse length $\kappa(\omega,T)$ increases with T and ω. As can also be deduced from Fig. 1, raising either T or ω increases $\kappa(\omega,T)$. Similar increases are associated with frequencies ω and temperatures T where $k_B T \approx \hbar\omega$. The inset of the figure which shows $\kappa(\omega,T)$ plotted against $\sqrt{T^2+(\hbar\omega/k_B)^2}$ makes this result more obvious. Here, the $\kappa(\omega,T)$ values for different ω's cluster near a single line with inverse slope 2000 $(\mathring{A}K)^{-1} \equiv \frac{1}{3}\frac{Ja_0}{k_B}$, where J is the exchange constant of pure La_2CuO_4.[6,15] Correspondingly, the solid curves in the inset and main body of the figure for which

$$\kappa^2 = \kappa_0^2 + a_0^{-2}((k_B T/E_T)^2 + (\hbar\omega/E_\omega)^2)^{1/Z} , \qquad (3)$$

$Z=1$, $\kappa_0 = 0.034\mathring{A}^{-1}$, and $E_T = E_\omega = 47\,meV \equiv \frac{1}{3}J$, give a good description of the data. It is physically appealing to interpret Eq. (3) as specifying the metric by which distances to a hypothetical quantum critical point at $T=0$, $\kappa_0=0$, and $\omega=0$ are measured in the three-dimensional phase space defined by T, κ_0 and ω (κ_0 is a sample-dependent parameter related to the doping level). Even though it is not obvious that such an analysis should apply to doped La_2CuO_4, we have chosen the form (3) because it is one of the

simplest possible descriptions of $\kappa(\omega,T)$ in the vicinity of a quantum critical point;[14] the exponents associated with T and ω are assumed to be the same because of theoretical arguments[15] that they should be the same for d=2. Since there are models (such as a popular treatment[16] of NMR in high-T_c materials) for which Z=2 rather than Z=1, we have also fitted the data using eq. (3) with Z=2. In Fig. 2, the dashed lines, evaluated (like the solid [Z = 1] lines) for $\hbar\omega$=6.1 and 15 meV, represent the less than perfect outcome of this procedure. That the solid lines follow the data more closely shows that for $La_{1.86}Sr_{0.14}CuO_4$, Z=1 has higher probability than Z=2. Indeed, allowing κ,Z,E_T and E_ω all to vary to yield the best fit gives $\kappa_o = 0.033 \pm 0.004 \mathring{A}^{-1}$, $E_T/k_B = 590 \pm 100$K, $E_\omega/k_B = 550 \pm 120$K and $Z = 1.0 \pm 0.2$.

We turn now to the peak amplitudes $\chi''_P(\omega,T)$. Fig. 3 shows how they and the Brillouin zone-averaged response functions $<\chi''> = \int \chi''(Q,\omega)\,d^2Q / \int d^2Q$ depend on ω for several temperatures. In agreement with our earlier work,[8] there is no statistically significant evidence for a spin gap or even a pseudogap at any $T \geq T_c = 35$K. Furthermore, only for the lowest T=35K, and here only when the peak - not integrated - response is considered, is there an identifiable energy scale below 15 meV. For 35K, the scale is the 7 meV energy transfer beyond which the peak spectrum flattens out. Otherwise, all data are in the low-ω regime where $\chi''_P(\omega,T)$ is proportional to ω. This means that at each T $\geq$ 85K, all of our measurements are characterized by a single amplitude parameter, namely $\chi''_P(\omega,T)/\omega$. Even for 35K $\leq$T$\leq$85K, this is true for $\hbar\omega$<5meV. We consequently shift our attention to the detailed T-dependence of $\chi''_P(\omega,T)/\omega$ and $<\chi''>/\omega$ both shown in Fig. 4(a). The remarkable result is that a $T^{-\alpha}$ law with

$\alpha = 1.94 \pm 0.06 \cong 2$ describes the rapid decrease of $\chi''_P(\omega,T)/\omega$ with increasing T. If we insist on a quantum critical description for $\chi''(Q,\omega)$, i.e. neglect κ_0^2 and rewrite eqs. (1) and (3) in a form which manifestly displays ω/T scaling,[7,17]

$$\chi''(Q,\omega) \approx \frac{a_1}{T^{(2-\eta)/Z}} \Phi \left[\frac{\sqrt{R}(Q)}{T^{1/Z}} , \frac{\hbar\omega}{k_B T} \right] . \qquad (4)$$

The result that $\alpha \cong 2$ implies $\eta = 2 - Z$. Because our analysis of the T- and ω-dependent inverse length scale $\kappa(\omega,T)$ favors $Z = 1$, the most likely value of η is 1. This pair of critical exponents is expected for 1-d quantum antiferromagnets (QAFM),[18] but is unanticipated[19] for 2-d QAFM, about which the general belief is that $Z = 1$ and $\eta \cong 0$.[15]

Nuclear relaxation measurements constitute a common probe of local magnetic response functions in the cuprates. We have therefore computed[20] the contribution of the incommensurate peaks observed using neutron scattering to the nuclear relaxation rates for $La_{1.86}Sr_{0.14}CuO_4$. Walstedt et al.[5] have already pointed out that at low T, the computed and observed rates for both copper and oxygen agree to within experimental error. However, Fig. 4(b) shows that warming yields a growing discrepancy between calculated and observed temperature dependences not only for the planar oxygen,[5] but also for the copper. At 250K the discrepancy corresponds to a Q-independent (or weakly Q-dependent) $\chi''(Q,\omega)/\omega$ of order 250 μ_B^2 / $(eV)^2$ for both copper and oxygen. Obviously, our unpolarized measurements, restricted to the region near (π,π) and insensitive to flat (on the scale of the experimental window) magnetic scattering, are entirely consistent with such a term. It is also possible that on warming, $\chi''(Q,\omega)$ acquires

MAY-29-1996 15:18 THEORETICAL PHYSICS 416 978 2537 P.17

substantial structures away from (π,π). Less probably, the extrapolation from the neutron (-3.5meV$\cong$40K) to nuclear resonance frequencies might become unreliable at high T due to the appearance of a thermally induced low-ω term.

To summarize, we have measured the Q- and ω- dependent magnetic response near (π,π) in $La_{1.86}Sr_{0.14}CuO_4$ from $T_c = 35$K to 350K and have obtained unexpectedly simple results. The response is dominated by incommensurate features whose widths can be described as rising in proportion to the temperature and energy transfer added in quadrature and whose peak intensities vary as T^{-2}. Finally, comparison between the neutron data and nuclear resonance results indicate a thermally-induced contribution to $\chi''(Q,\omega)$ which is not sharply peaked near (π,π).

Acknowledgements:

We thank B. Batlogg, P. Littlewood, A. Millis, D. Pines, S. Sachdev, B. Statt, and R. Walstedt for many helpful conversations, K.N. Clausen, K. Bechgaard, and J. Kjems for hospitality at Risó, and ECLIP, EPSRC, NSERC, CIAR, and USDOE for support.

MAY-29-1996 15:18 THEORETICAL PHYSICS 416 978 2537 P.18

REFERENCES

1. B. Batlogg et al., p.5 in *Electronic Properties of High-T_c Superconductors* (Springer, Berlin 1993).

2. F. Slakey et al., Phys. Rev. B. *43* 3764 (1991); Z. Schlesinger et al., Phys. Rev. Lett. *65* 801 (1990).

3. T. R. Chien et al., Phys. Rev. Lett. *67* 2088 (1991).

4. T. Imai, PhD thesis, University of Tokyo, 1991 (unpublished); T. Imai et al., J. Phys. Soc. Jpn. *59* 3846 (1990).

5. R. E. Walstedt et al., Phys. Rev. Lett. *72* 3610 (1994).

6. See review by D. C. Johnston, J. Magn. Magn-Mat. *100* 218 (1991).

7. S. M. Hayden et al., Phys. Rev. Lett. *66* 821 (1991); B. Keimer et al., Ibid *67* 1930 (1991); B. Sternlieb et al., Phys. Rev. B*47* 5320 (1993); Y. Zha et al., Physica C *212* 413 (1993); J. Rossat-Mignod et al., Physica B *169* 58 (1991); J. Ruvalds et al., Science *256* 1664 (1992).

8. M. Matsuda et al., Phys. Rev. B *49* 6958 (1994); T. R. Thurston et al., Ibid *46* 9128 (1992); T. E. Mason et al., Phys. Rev. Lett. *68* 1414 (1992); S.-W. Cheong et al., Ibid *67* 1791 (1991).

9. D. Vaknin et al., Phys. Rev. Lett. *58* 2802 (1987).

MAY-29-1996 15:18 THEORETICAL PHYSICS 416 978 2537 P.19

10. T. E. Mason et al., Phys. Rev. Lett. *71* 919 (1993).

11. H. Sato and K. Maki, Int. J. Magn. *6* 183 (1974); D. R. Noakes et al., Phys. Rev. Lett. *65* 369 (1990).

12. We have used acoustic phonons in scans along $Q=(2,\xi,0)$ and $(2,0,\nu)$ (orthorhombic notation) for $\hbar\omega=2$ and 2.7 meV (sound velocity $\equiv 23\,\mathrm{meV}-\mathring{A}$).

13. S. M. Hayden et al., Phys. Rev. Lett. *67* 3622 (1991); R. R. P. Singh et al., Phys. Rev. Lett. *62* 2736 (1989).

14. See overview by M. Continentino, Physics Reports *39* 179 (1994) and experiments by M. C. Aronson, et al., preprint (1994) and H. v. Löhneysen et al., Phys. Rev. Lett. *72* 3262 (1994).

15. S. Sachdev and J. Ye, Phys. Rev. Lett. *69* 2411 (1992); A. Chubukov et al., Phys. Rev. B *49* 11919 (1994); A. J. Millis, Phys. Rev. B *48* 7183 (1993).

16. A. J. Millis et al., Phys. Rev. B *42* 167 (1990); T. Moriya et al., J. Phys. Soc. Jpn. *59* 2905 (1990).

17. C. M. Varma et al., Phys. Rev. Lett. *63* 1996 (1989).

18. A. Luther and I. Peschel, Phys. Rev. B *12* 3908 (1975).

19. Strongly interacting *fermions* in 2-d could in certain respects behave as in 1-d. See, e.g. P. W. Anderson, Phys. Rev. Lett. *64* 1839 (1990), L. Ioffe et al., Phys. Rev. Lett. *73* 472 (1994), and A. Luther, Phys. Rev. B *50* 11446 (1994).

MAY-29-1996 15:19 THEORETICAL PHYSICS 416 978 2537 P.20

20. We have followed ref. [5] and used the formulae $^{63}(T_1T)^{-1} = 2\gamma_{Cu}^2 k_B \hbar \langle (A+2B(\cos q_x a_o + \cos q_y a_o))^2 \chi''(Q,\omega)/\omega/g^2 \rangle$ and $^{17}(T_1T)^{-1} = 4\gamma_O^2 k_B \hbar \langle (C_a^2 + C_b^2)\cos^2 q_x a_o \chi''(Q,\omega)/\omega/g^2 \rangle$ where $\chi''(Q,\omega)$ is the periodic function defined as the sum over copies of eq. (1) where the arguments Q have been shifted by all (square) reciprocal lattice vectors, <...> denotes averages over the Brillouin zone and $g=2.06$, $\gamma_{Cu} = 2\pi \times 1.1285 \times 10^3$ (sec-G)$^{-1}$, $\gamma_O = 2\pi \times 0.5772 \times 10^3$ (sec-G)$^{-1}$, $A = 18 \times 10^3$ G/spin, $B = 92 \times 10^3$ G/spin, $C_a = 108 \times 10^3$ G/spin, and $C_b = 64 \times 10^3$ G/spin. See also F. Mila and T. M. Rice, Physica C *157* 561 (1989), and B. Shastry, Phys. Rev. Lett. *63* 1288 (1989).

FIGURE CAPTIONS

Fig. 1 (a) Constant $\hbar\omega = 6.1$ meV scans through two incommensurate peak positions. Actual counting times were in the 10 to 60 minute per point range. Open symbols represent background collected along upper left-hand edge of colored area in (b). Solid lines correspond to resolution-corrected structure factor defined by eq. (1).

(b) 2-d reciprocal space, with color map of background-corrected intensity for $\hbar\omega = 6.1$ meV. Above the diagonal ($\xi \simeq \beta$), the map is derived from three scans between the (π,π) direction and the background scan shown at right in (a). Below the diagonal, the map shows the resolution-corrected structure factor (eq. (1)) with parameters $\kappa = 0.15\text{Å}^{-1}$ and $\chi''_P(\omega,T) = 10.5\mu_B^2/\text{eV}$ chosen to best describe the data above the diagonal.

(c) - (e) Energy and momentum (along solid trajectory in (b)) -dependent magnetic response function $\chi''(Q,\omega)$, derived from raw data using fluctuation -dissipation theorem. No attempt has been made to correct for experimental resolution, which broadens and weakens sharp features in $\chi''(Q,\omega)$. Color scale indicates $S(Q,\omega)$ for the three temperatures while the (vertical) numerical scales are in units of counts/6 min /$(n(\omega) + 1)$.

Fig. 2 Temperature dependence of inverse length scales $\kappa(\omega,T)$ at various fixed energy transfers $\hbar\omega$. Solid and dashed lines correspond to $Z = 1$ and $Z = 2$ quantum critical points, respectively (see eq. (3) and text). Inset shows $\kappa(\omega,T)$

MAY-29-1996 15:19 THEORETICAL PHYSICS 416 978 2537 P.22

replotted against T and $\hbar\omega$ added in quadrature. Solid line is described in text.

Fig. 3 Energy dependence of (a) averaged (over full Brillouin zone, using periodic generalization of eqs. (1) and (2)) and (b) peak response at various temperatures. Triangles are derived from a constant-Q scan at an incommensurate peak while diamonds and closed symbols are the amplitudes $\chi_P''(\omega,T)$ obtained, using the fits described in text, from constant - $\hbar\omega$ scans.

Fig. 4 Temperature dependence of (a) Brillouin zone-averaged (see caption for Fig. 3) and resolution-corrected peak response derived from fits to neutron data and (b) nuclear relaxation rates for ^{63}Cu and planar ^{17}O derived from neutron scattering data (solid symbols) and actually measured[4,5] (open symbols). Solid lines in (a) and (b) are calculated using eqs. (1), (2), and (3) with $\chi_P''(\omega,T)/\omega \sim T^{-1.94}$, $E_T = E_\omega = 47$ meV, $Z = 1$, and $\kappa_0 = 0.034\,\text{Å}^{-1}$. Absolute scale in (a) is from normalization to phonons.[12] In view of uncertainties in both the nuclear relaxation and neutron experiments as well as the hyperfine Hamiltonian, we have fixed the absolute scale in (b) by equating the computed and observed ^{63}Cu rates at 35K.

MAY-29-1996 15:19 THEORETICAL PHYSICS 416 978 2537 P.23

a)
T=80 K
T=297 K
ΔE=6.1 meV
Q=ξ(π,π)+(δ/√2)(-π,π)
Intensity (Counts/6 min)
ξ
b)
T=297 K
ΔE=6.1 meV
ζ(0,π)
η(π,0)
c)
T=35 K
χ''
Energy (meV)
d)
T=80 K
χ''
Energy (meV)
e)
T=297 K
χ''
Energy (meV)

FIGURE 1

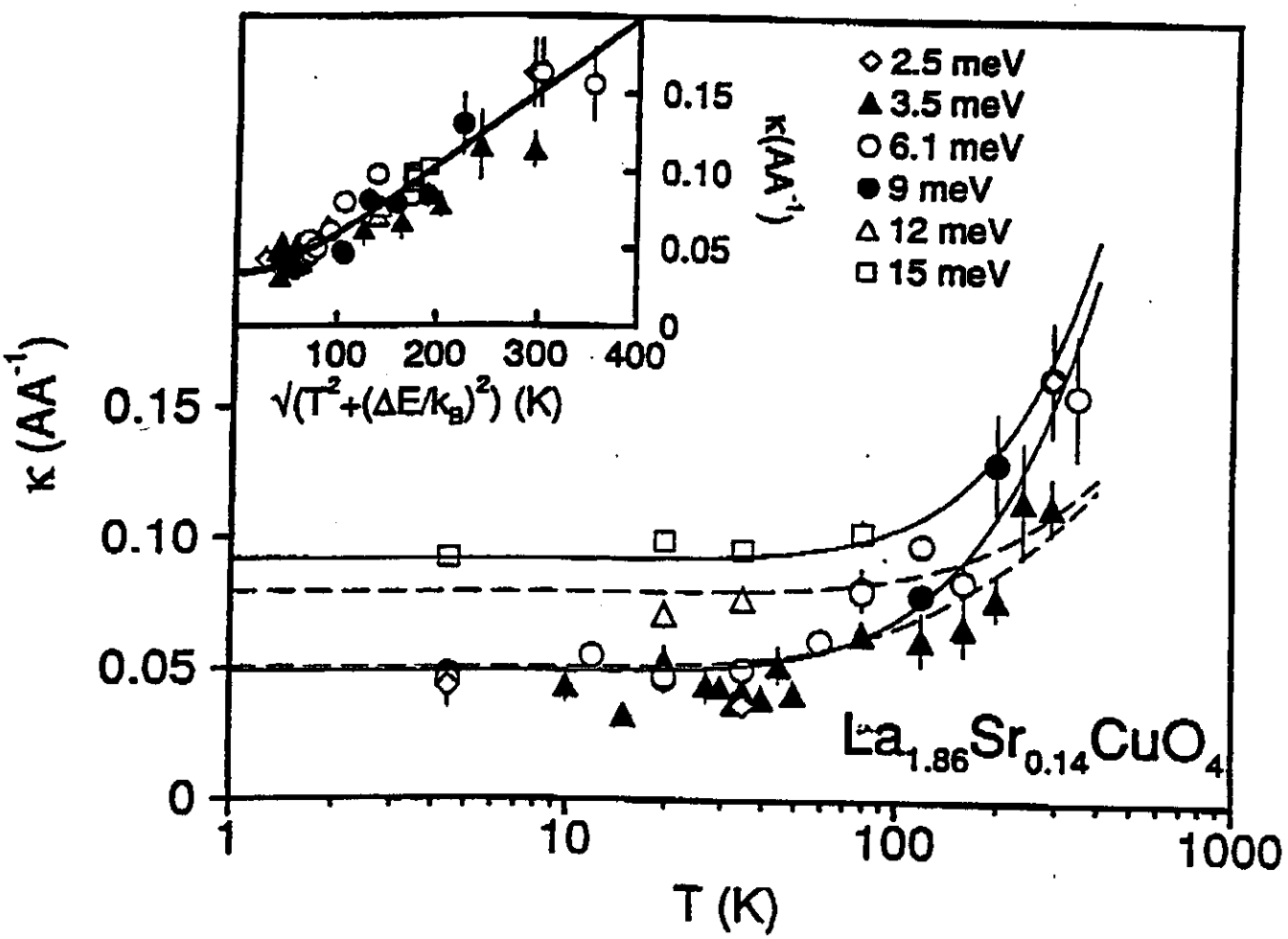
κ (AA^{-1})
0.15
0.10
0.05
0
1
10
100
1000
T (K)
◇ 2.5 meV
▲ 3.5 meV
○ 6.1 meV
● 9 meV
△ 12 meV
□ 15 meV
La$_{1.86}$Sr$_{0.14}$CuO$_4$
κ(AA^{-1})
0.15
0.10
0.05
0
100
200
300
400
$\sqrt{(T^2+(\Delta E/k_B)^2)}$ (K)

FIGURE 2

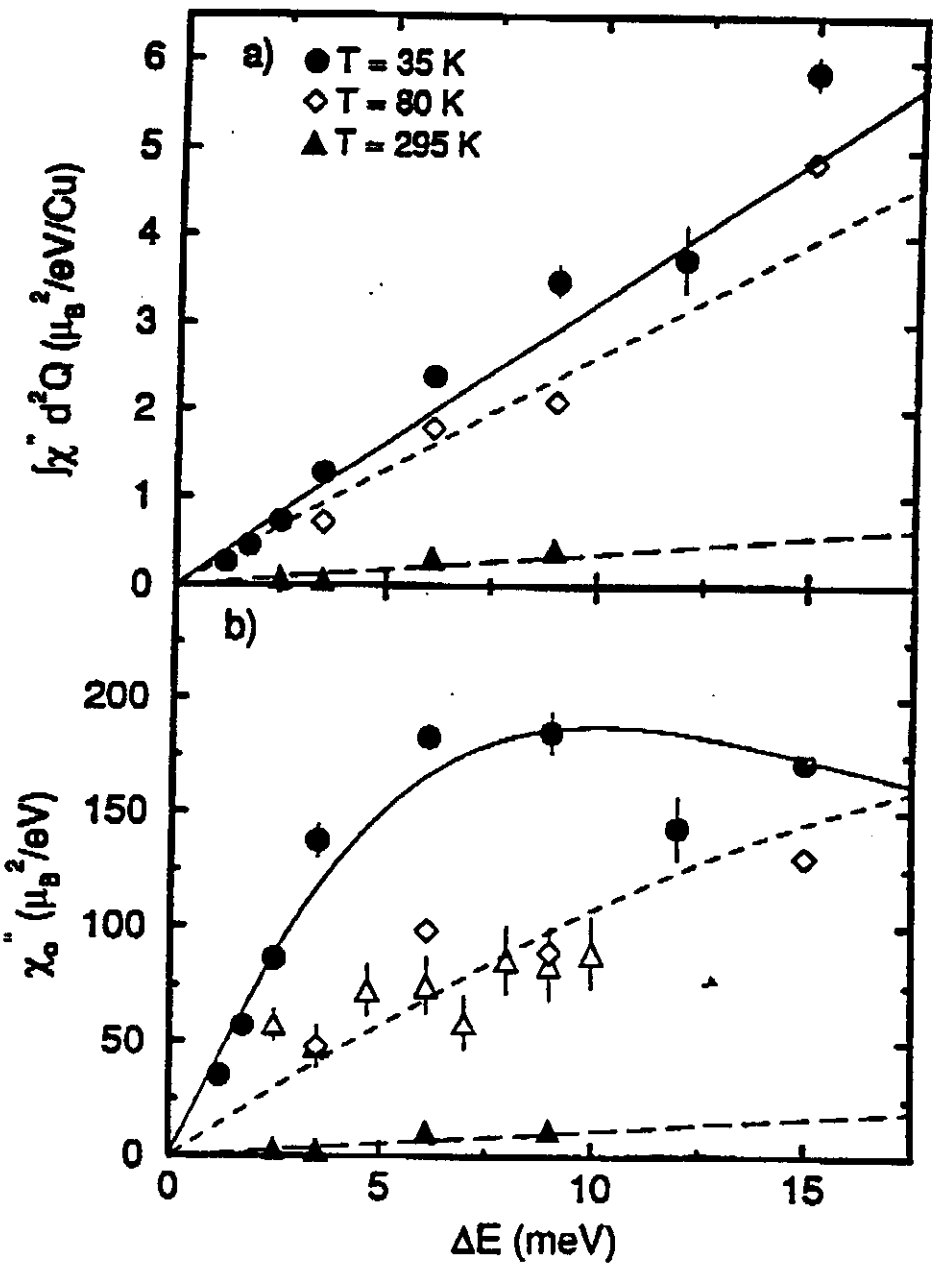

FIGURE 3

a)
$La_{1.86}Sr_{0.14}CuO_4$
$\int\chi''d^2Q/\omega, \chi_o''/\omega\ (\mu_B^2/eV^2)$
$\chi''(Q_o)/\omega$
$\int\chi''d^2Q/\omega$
b)
$(T_1T)^{-1}\ (sec^{-1}K^{-1})$
^{63}Cu (Imai)
^{63}Cu (Walstedt)
^{63}Cu (Neutrons)
$10^{*17}O$ (Walstedt)
$10^{*17}O$ (Neutrons)
T(K)

FIGURE 4